

Experimental investigation of rheological properties and formation damage of water-based drilling fluids in the presence of Al₂O₃, Fe₃O₄, and TiO₂ nanoparticles

Pedram Ejtemaee¹ , Ehsan Khamsehchi^{1,*} 

¹Department of Petroleum Engineering, Amirkabir University of Technology (Tehran Polytechnic), Tehran, Iran

²Department of Petroleum Engineering, Amirkabir University of Technology (Tehran Polytechnic), Tehran, Iran

*corresponding author e-mail address: khamsehchi@aut.ac.ir | Scopus ID [26657370700](https://orcid.org/0000-0001-9142-1000)

ABSTRACT

The successful drilling of the oil and gas wells almost relies upon the drilling fluid properties. Maintaining wellbore stability, transportation, and releasing cuttings at the surface, and controlling formation pressure are the essential functions of the drilling fluid. Improving the rheological properties of the drilling fluid results in an increase in transport power and also provides better stability. One of the new methods to improve different properties of the drilling mud is the application of nanoparticles. Nanoparticles induce favorable effects on the rheological properties of the fluid. Improvement of mud properties yields in better cleaning of the well, the stability of the wellbore, higher drilling bit efficiency, and, consequently, a lower cost in the long run. Therefore, the present study investigates the effect of adding three different nanoparticles including aluminum oxide, iron oxide, and titanium oxide to the drilling fluid in several experiments by measuring rheological properties (plastic viscosity, yield point, filtration rate, gel strength) and also formation damage and permeability reduction. The number of experiments was determined by the experiment design method. The results of the experiments implied that in nanofluids with the weight of 70 pcf, rheological properties were relatively improved in most of the nanofluids samples concentrations. Samples containing iron oxide exhibited a decreasing filtration rate compare to base drilling fluid that indicates increasing stability in the fluid environment. The gel strength (GS) of titanium oxide and aluminum oxide samples has increased appropriately, which shows improvement in attractive forces in the fluid. For the case of the 80 pcf nanofluid, iron oxide indicates appropriate rheological properties and decreasing of filtration rate that all of them represent nanoparticle caused an increasing and improving the stability of fluid. But titanium oxide and aluminum oxide couldn't show significant effects. This phenomenon can be described by the lack of a uniform and thorough mixing of nanoparticles in the drilling fluid under field conditions. Besides, results obtained from the formation damage test equipment demonstrated the 54% reduction in initial permeability of the iron oxide nanoparticle that is the lowest damage between another nanofluid.

Keywords: *Drilling fluid; nano-particle; experiment design; formation damage; rheology properties.*

1. INTRODUCTION

By definition, a Nano-Particle (NP) is a particle with a diameter of about 1 to 2 nm. In addition to the metallic type, insulators, and semiconductors, the NPs also incorporate synthetic NPs such as core structures. Moreover, nanospheres, nanomaterials, and nanofibers are other forms of NPs. NPs low in size are known as nanoclusters. Nanocrystals and semiconductor quantum dots are also subsets of NPs. In recent years, NPs have been extensively used in different areas such as electronic, electrical, medicine, space and information, science and engineering [1-6].

Drilling mud has a significant role in accelerating or delaying drilling operations. This fluid has many functions in drilling operations, such as transferring drilling cuttings to the surface, keeping the drill bit cool, preventing the wall from falling, controlling the formation pressure, and pumping hydraulic power to the drill without which drilling operations would not be possible.

Properties such as hydraulic power transferability and compressibility are among the most critical factors that appear to be achievable through the use of nanocomposites, carbon nanotubes, and some high-strength ceramic nanopowders of appropriate weight (such as calcium carbide nanopowders). The drilling mud must also have properties such as suitable viscosity and density for efficient carrying drilling cuttings upwards as well as transferring the hydraulic power transferability of the pumps. It is possible to

achieve the properties required from the drilling mud by adding specific chemicals, such as polymers, thickeners, etc. Proper viscosity is also achieved by adding lubricating nanofluids. Properties such as hydraulic power transferability and compressibility are among the most important factors that appear to be achievable through the use of nanocomposites, carbon nanotubes, and some high-strength ceramic nanopowders of appropriate weight (such as calcium carbide nanopowders). The thixotropic properties of a drilling mud can also be improved by nano-additives. If the drilling operation is interrupted, the mud should be gelatinized, preventing the drilling cuttings from settling down and preventing the drilling cuttings from getting into the well. The gelatinous mud should also be in a state of low gelatinous stress and restore the thixotropic property of the mud. In this regard, the use of nanomaterials has a significant effect on improving these properties.

Choosing a convenient drilling fluid formulation for specific drilling conditions has a crucial role in the succession of drilling operations, particularly in unconventional formations. The need for enhanced drilling fluids has led researchers to investigate the development of improved drilling fluids, using various NPs as additives [7, 8]. Nanotechnology has been applied successfully in some cases like reservoir characterization, drilling and completion

jobs [9-14]. The application of nanotechnology in drilling fluid formulation has also been provided in the literature briefly [15-19].

Some researchers have reported the modeling of the rheology of nano-enhanced drilling fluids, as a function of shear rate, the volume fraction of NPs, and temperature, parameters which are critical toward high-fidelity computational modeling for producing cost-effective drilling fluids [20-22]. Li *et al.* [23] developed self-assembled silver NPs with an average size of 5 nm and incorporated the NPs in kerosene-based fluids. They conducted thermal conductivity measurements at three different temperatures (25, 40, and 50 °C). The results showed that the thermal conductivity of each silver nanofluid was higher than that of its base fluid and increased nonlinearly with increasing the concentration of the NPs.

Kang *et al.* [24] developed and studied water and oil-based drilling fluids containing silica NPs by running tests such as spontaneous imbibition, swelling rate, and acoustic transit time. Their results demonstrated that for the water-based drilling fluids, NPs led to higher Plastic Viscosity (PV) and Yield Point (YP), and lower API-filtration. They attributed this behavior to the fact that silica NPs can quickly disperse in the water-based fluids and effectively prevent the filtration into shale by plugging pore throats. However, it is not easy for NPs to disperse in oil-based fluids, thus reducing their effectiveness.

Ismail *et al.* [25] investigated the use of Multi-Walled Carbon Nanotubes (MWCNTs) as an additive to improve the rheological properties of water-based and ester-based drilling fluids. They focused on finding the optimum concentration of MWCNTs with an average diameter of 30 nm to induce better rheological properties at various temperatures. The results indicated that the concentrations of MWCNTs that were used in the water-based drilling fluid do not much affect PV, YP, and GS. Alizadeh *et al.* [26] studied the rheological behavior of a drilling mud

containing alumina/polyacrylamide nanocomposite. The synthetic nanocomposite was prepared through the solution polymerization method. They noticed that the viscosity of the drilling fluid increased up to more than 300 cp for both freshwater and brine-based mud by adding 4% of the nanocomposite. Furthermore, they indicated that the nanocomposite tested was able to reduce the thixotropy of the produced drilling fluid.

Amarfio *et al.* [27] evaluated the impact of Al_2O_3 NP on the rheological properties of water-based mud. The results showed that Al_2O_3 NP provided thermal stabilization for the drilling mud under high-temperature conditions and that the Al_2O_3 NPs were able to maintain the shear stresses of the fluid as temperature rises. Parizad *et al.* [28] investigated the effects of SiO_2 NP and KCl salt on filtration and thixotropic behavior of polymeric water-based drilling fluid in different concentrations and temperatures with zeta potential and size analysis. They reported that the SiO_2 NP addition mostly improved the drilling fluid performance; however, the addition of SiO_2 NPs in higher concentrations was not much effective. The amount of SiO_2 NPs for valid and justifiable usage should be carefully selected. The KCl also effected SiO_2 NPs behavior in drilling fluid.

Over the past few years, the need for improved drilling fluids has led researchers to explore the development of advanced drilling fluids using different types of NPs as additives. Despite the relatively large number of studies on the effect of NPs on drilling fluid, there is a lack of studies regarding the effect of simultaneous NPs in laboratory and field conditions with an industrial application approach. In this paper, the effect of three different types of NPs on the rheological properties of drilling fluid and the extent of formation in both laboratory and field conditions is investigated with consideration of industrial applications and applications in two different weights, which is discussed in detail below.

2. MATERIALS AND METHODS

2.1. Drilling and nanofluid materials.

In this study, the base drilling fluid included water, Soda Ash (as water hardness reducer), Sodium Chloride Salt (as weighting agent), Lime (as pH control), and Natural Gum (as viscosifier). All of these materials were purchased from Aharan Group Company. Three NPs (Fe_3O_4 , Al_2O_3 , TiO_2) were added to the base drilling fluid to investigate the rheology properties and formation damage of these nanofluid. The properties of the NPs which were purchased from Tamad Kala are given in Table 1.

2.2. Core samples and saturation water.

The cores in this study were obtained from carbonate outcrop rock of south of Iran, and before using they were cleaned by methanol and were arid. Properties of cores are shown in table 2. For saturating the cores, 5% w/w of potassium chloride solution was used.

2.3. Drilling fluid preparation.

A stepwise procedure was used to prepare the base mud (a drilling fluid with a weight of 70 pcf). The base drilling fluid preparation began with adding NaCl to water and mixing for 15 minutes. After that, soda ash was used to eliminate the hardness of the water. Next, lime and natural gum were added. Finally, the prepared solution of NPs in distilled water was combined with the sample.

Before each drilling fluid additive was included, the sample was mixed with an American Hamilton Beach Mixer for 15-20 minutes to ensure uniform dispersion of the additives. After preparing the base fluid, an Ultrasonic Probe Device was used for mixture nano solution about 30 min to make sure the fluid be uniform. After the preparation of nanofluids due to simulating field conditions, samples were warm up in the rolling oven to 200 degrees Fahrenheit. Then rheological properties of samples were measured by Fann 35 VG-meter, and an API100 filter press was used to measuring the drilling fluid filtration. Eventually, for measuring formation damage of three nanofluids that included TiO_2 , Al_2O_3 , and Fe_3O_4 , a formation damage measuring device (Vinci Technologies- FDS350) was used.

Also, similar steps have been taken to prepare a drilling fluid with a weight of 80 pcf as another base mud. The fluid preparation steps for the base muds with 70 and 80 pcf are mentioned in Table 3 and Table 4, respectively. This study aimed to investigate the rheological properties and formation damage of water-based mud, including three different NPs of iron oxide (Fe_3O_4), aluminum oxide (Al_2O_3), and titanium oxide (TiO_2) at four different concentrations.

Times experimental investigation of rheological properties and formation damage of water-based drilling fluids in the presence of Al₂O₃, Fe₃O₄, and TiO₂ nanoparticles

Table 1. The physical properties of the used NPs.

NP	Purity (%)	Dimension (nm)	specific surface area (m ² /g)
Iron Oxide (Fe ₃ O ₄)	99.0	20-30	60
Aluminum Oxide (Al ₂ O ₃)	99.0	20	>138
Titanium Oxide (TiO ₂)	99.5	40	35

Table 2. The Properties of cores.

Core	Length (cm)	Diameter (cm)	Porosity (%)	permeability (md)
1	10.6	3.8	24.6	61.28
2	9.6	3.8	23.7	61.28
3	8	3.8	25.2	73.54

Table 3. Fluid preparation steps for the base mud (70 pcf).

NO	Sample	Water (cc)	NaCl (g)	Soda Ash (g)	Lime (g)	Natural Gum (g)	NPs (g)
1	Base	325	66.000	1.000	0.800	8.000	0.000
2	Al ₂ O ₃	275	66.000	1.000	0.800	8.000	0.050
3	Al ₂ O ₃	275	66.000	1.000	0.800	8.000	0.100
4	Al ₂ O ₃	275	66.000	1.000	0.800	8.000	0.500
5	Al ₂ O ₃	275	66.000	1.000	0.800	8.000	1.000
6	TiO ₂	275	66.000	1.000	0.800	8.000	0.050
7	TiO ₂	275	66.000	1.000	0.800	8.000	0.100
8	TiO ₂	275	66.000	1.000	0.800	8.000	0.500
9	TiO ₂	275	66.000	1.000	0.800	8.000	1.000
10	Fe ₃ O ₄	275	66.000	1.000	0.800	8.000	0.100
11	Fe ₃ O ₄	275	66.000	1.000	0.800	8.000	0.500
12	Fe ₃ O ₄	275	66.000	1.000	0.800	8.000	1.000
13	Fe ₃ O ₄	275	66.000	1.000	0.800	8.000	1.500

Table 4. Fluid preparation steps for the base mud (80 pcf)

NO	sample	Water (cc)	NaCl (g)	Soda Ash (g)	Natural Gum (g)	Limestone Powder (g)	NPs (g)
1	Base	325	66.000	0.500	8.000	107.000	0.000
2	Al ₂ O ₃	275	66.000	0.500	8.000	107.000	0.050
3	Al ₂ O ₃	275	66.000	0.500	8.000	107.000	0.100
4	Al ₂ O ₃	275	66.000	0.500	8.000	107.000	0.500
5	Al ₂ O ₃	275	66.000	0.500	8.000	107.000	1.000
6	TiO ₂	275	66.000	0.500	8.000	107.000	0.050
7	TiO ₂	275	66.000	0.500	8.000	107.000	0.100
8	TiO ₂	275	66.000	0.500	8.000	107.000	0.500
9	TiO ₂	275	66.000	0.500	8.000	107.000	1.000
10	Fe ₃ O ₄	275	66.000	0.500	8.000	107.000	0.100
11	Fe ₃ O ₄	275	66.000	0.500	8.000	107.000	0.500
12	Fe ₃ O ₄	275	66.000	0.500	8.000	107.000	1.000
13	Fe ₃ O ₄	275	66.000	0.500	8.000	107.000	1.500

2.4. Rheology and filtration measurement.

Firstly, the 70 and 80 pcf water-based muds were prepared and then NPs were added in a suspension state with predetermined concentrations (Figure 1). Then, the corresponding rheologic properties and formation damage were measured. Some points were considered for the tests with the 70 and 80 pcf muds including determination of the mud weight. Considering the specific needs for utilizing the oil-based mud, shale problems, formation damage, and consequently, the significant rise in the drilling costs of reservoir formation, it was decided to test an interval of muds' weight which owns the most common applications. Initially, a 70 pcf water-based mud was prepared, and after adding three NPs, it was separately tested for four different concentrations in the samples. All the rheological properties of the drilling fluid were measured. The base mud containing no NPs was used as an index for comparison.

A total of thirteen tests were performed for thirteen different mud samples. The rheological properties including, PV, YP, FR, and GS were measured. In the preparation of the 70 pcf mud, the only salt was utilized to increase the mud's weight and natural gum as viscosifier. This allowed us to observe the mere effects of NPs on the fluid properties as the reactivity of the nanoparticles highly promotes due to the increase in the effective surface area, consequently, the addition of any other material may influence the NPs' performance. At all stages of the tests with the 70 pcf mud, laboratory standards such as the use of ordinary water, ultrasonic mixers to process the nano-particle solution, and adjusting the drilling fluid pH to 11 were considered. The real conditions of the oil field were applied for the tests with the 80 pcf mud. As the second stage of tests, an 80 pcf base mud was considered to make sure it would provide enough hydrostatic pressure to surpass the formation pressure. For this heavier mud,

field considerations were mostly followed such as using the local water and setting the pH on 7.5 and incorporating the Hamilton Beach mixer with its highest speed in preparing the base mud and also the NPs suspension fluids.

The test for determining the formation of damage is highly time-consuming. Hence, just the optimum concentrations of the NPs previously determined in other tests regarding the rheologic properties were considered. The optimum concentration values for the Fe_3O_4 , Al_2O_3 , and TiO_2 were 0.28, 0.14, and 0.028 wt%, respectively.

During all the three tests, three identical cores with certain dimensions were placed in the device. Initially, the initial permeability was recorded, then, the test was continued in dynamic

and static modes, each for three hours, and finally, the permeability of the core was recorded after the formation damage test.



Figure 1. Prepared samples for drilling nanofluids.

3. RESULTS

3.1. The 70 pcf sample.

3.1.1. Plastic Viscosity (PV).

Figure 2 shows the effect of adding different NPs on the PV of the drilling fluid samples at different concentrations for the 70 pcf mud. The Al_2O_3 NP viscosity graph suggests that the viscosity of all NP mud samples is higher than that for the base mud, which is physically justifiable. According to this figure, the PV increases have an ascending trend to the concentration of 0.15 wt.% and then decreases. This decrease can be attributed to the increase in concentration, disruption of the suspension solution stability, and consequently, the precipitation and deposition of the particles. In the case of Fe_3O_4 NP, it can be said that at concentrations less than 0.07 wt.%, the NP did not have a particular effect on the fluid, in fact, it has caused a decrease in the PV by destabilizing the fluid. Between the concentrations of 0.07 to 0.24 wt%. the PV shows a normal behavior. the PV has increased by increasing the number of bonds due to the increase of NPs and electric charges and then decreasing so that the decrease after 0.24 wt% decrease the viscosity is lower than the base mud. It becomes stable and stable from 0.3% wt. The graph for the TiO_2 NP indicates that in the mud sample at concentrations below 0.14 wt% PV is lower than that for the base mud and the NP concentrations up to 0.1 wt% have adverse effects on the properties of the muds. The increases in the electrochemical charges in the fluid result in precipitation and deposition of the solid particles, which has decreased the PV. However, after the 0.14 wt% concentration, the PV surpasses that for the base mud and continue its ascensive trend.

3.1.2. Yield Point (YP).

It assumed that the increase in NPs concentration causes to increase the yield point (YP) such as PV, due to the increased charges in the mud. Figure 3 shows the effect of different NPs on the YP of the drilling fluid samples. According to this figure, in the case of Al_2O_3 NPs, it can be expressed that the YP for the NP-contained mud is higher than that for the base mud throughout the testing process. It indicates an increase in the attraction forces inside the mud induced by NPs addition. The value of YP increased until the Al_2O_3 concentration reach to 0.14% by weight, but it decreased from this point onwards. It can be assumed that the further addition of NPs causes the electrical charge neutralization in the fluid, and the yield point could make the fluid more stable by reducing itself [29]. The investigation of the graph obtained from the experimental

data on the Fe_3O_4 NP sample shows an ascending trend throughout the testing path. The path confirms the prediction, and the increase in the concentration of Fe_3O_4 NPs increased the electrochemical charges in the mud, which resulted in YP increasing. At concentrations below 0.25 wt. %, YP is lower than that for the base mud; in fact, this amount of NP concentration has neutralized the extra electrical charges, and higher NP concentration has kept the YP constant at that of base mud and has stabilized it. According to the TiO_2 NP diagrams, the NPs maintain mud stability at all concentrations, and the electrical charge changes were not such as to cause a gap in the drilling fluid properties, and the rheological properties remained unchanged.

3.1.3. Filtration Rate (FR) and mud cake.

The filtration rate (FR) of the various samples shown in Figure 4. Water loss of mud at all concentrations of Al_2O_3 NPs was higher than that for the base mud, indicating a lack of formation of stable structure within the drilling mud. The reason for this is the sizeable molecular-scale particle size, which causes form the larger bonds; therefore, the low-permeability mud cake does not develop. The thickness of the mud cake was not measurable due to the unstable cake.

In the Fe_3O_4 NP mud sample, based on the FR diagram and mud cake thickness, stronger bonds formed, the cake quality increased, resulting in a gradual decrease in the water loss of the mud as the concentration of the NP increased. For samples made with TiO_2 NPs, as can be seen in the figure, the FR and mud cake thickness values are between that for two previously mentioned NP-contained mud samples. It indicates relatively good bonds between the NPs and the drilling fluid components [29]. FR remained almost constant with the gradual increase of TiO_2 NPs concentration, and it began to decrease at the concentration of 0.15 wt. %, indicating improved fluid rheological properties. The mud cake also did not fluctuate and showed the same thickness at all concentrations.

3.1.4. Gel Strength (GS).

As mud additives increase the gravity forces inside the mud, the amount of mud gel strength (GS) will increase. According to Figure 5, which shows the effect of different NPs concentration on the GS of the drilling fluid, the GS was initially almost constant with the increase in Al_2O_3 NP concentration, indicating the general stability of the drilling fluid. Then, the GS increased with a slight

trend due to the increase in positive and negative charges inside the mud.

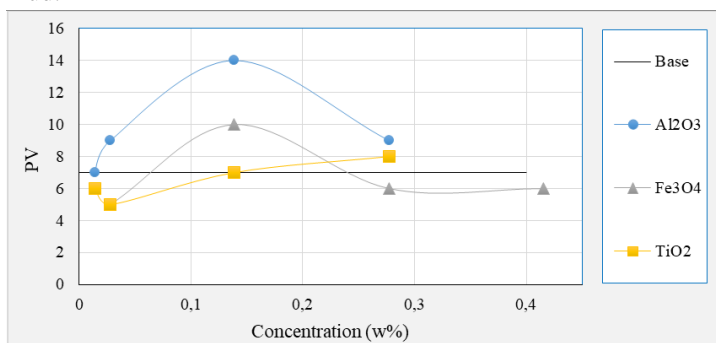


Figure 2. Effect of different NPs concentration on PV of drilling fluid sample in different concentrations (70 pcf sample)

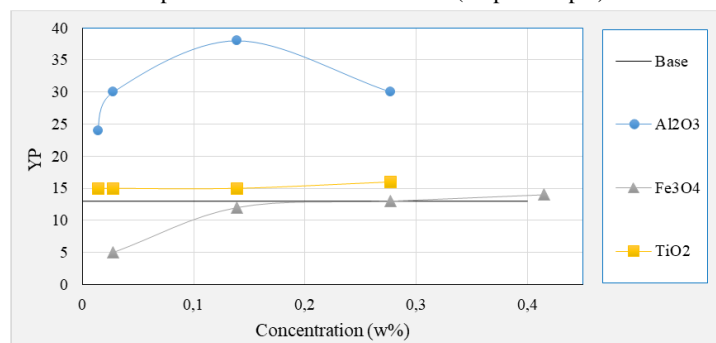


Figure 3. Effect of different NPs concentration on the drilling fluid sample variation in different concentrations (70 pcf sample)

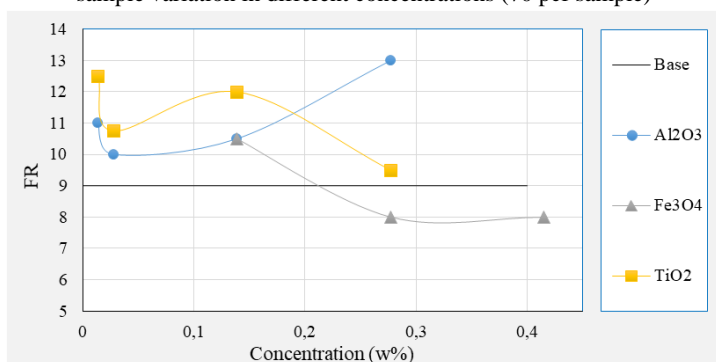


Figure 4. Effect of concentration of different NPs on FR of drilling fluid sample in different concentrations (70 pcf sample)

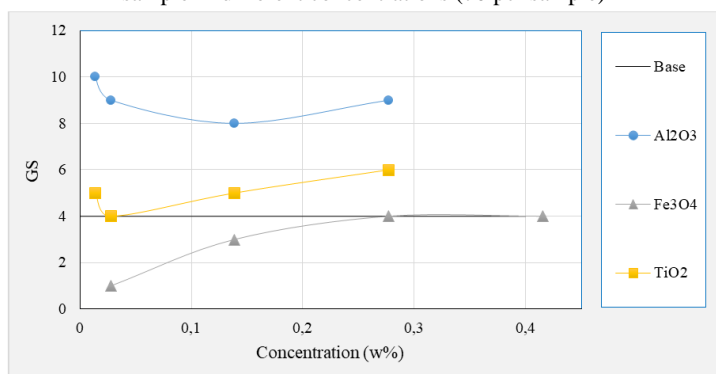


Figure 5. Effect of different NPs concentration on GS of drilling fluid sample in different concentrations (70 pcf sample)

It can be seen in the Fe₃O₄ NP diagram that although the GS of the Fe₃O₄ NP-containing mud was initially lower than that for the base mud, with the increase in Fe₃O₄ NP concentration, the GS increased gradually. This gradual increase is due to the increase in electrical charges and stronger bonding. The TiO₂ NP diagram shows that, at all concentrations, the amount of GS was slightly higher than that for base mud, but no significant changes observed.

3.2. The 80 pcf sample.

3.2.1. Plastic Viscosity (PV).

PV reflects the collision of particles in the fluid. The Al₂O₃ NP-containing sample has a lower PV than the base mud, indicating that the addition of Al₂O₃ NP up to a concentration of 0.02 wt. % caused an increase in the viscosity, but the higher NP concentration disrupted the fluid equilibrium. With the accumulation and deposition of particles, the number of collisions has decreased, which reduces the ability of drilling fluid to suspend and carry the drilling cuttings. Of course, this decline is not very significant.

In the Fe₃O₄ NP-containing mud sample, the rheological properties do not alter up to NP concentration of 0.025 wt. %, and then the viscosity increases concerning NP concentration. It means that the drilling fluid properties improve for the suspending and transfer of the drilling cuttings. Investigation of the TiO₂ NP-containing mud diagram indicates that the viscosity increases up to an NP concentration of 0.02 wt. % and then decreases to a fixed value. It means that the increase of NP concentration up to 0.02 wt. % causes to improve the bonds inside the fluid. Still, with more increase in NP concentration, the equilibrium is lost, and the rheological properties slightly decreased, while the stability of drilling fluid preserved (Figure 6).

3.2.2. Yield Point (YP)

To analyze the YP diagram, it is essential to note that the ascending or descending trends of the diagram are not a positive or negative criterion for the effect of NPs addition, but when the YP is in the normal range or the changes cause the diagram to move in the normal direction, it reveals a positive effect and indicates fluid stability. Excessive increase in YP causes the drilling fluid to become a gel and put extra pressure on the mud pump. On the other hand, excessive reduction in YP also reduces the ability of drilling fluids to remove cuttings. The increase in Al₂O₃ NPs initially caused to reduce YP, and its value is kept at about the same value as the base mud. It means that, up to Al₂O₃ NPs concentration of 0.14 wt. %, the NPs neutralized the excess soluble charge. Then a further increase of NPs concentration caused the internal attraction in drilling fluid and thereby YP increase. According to Figure 7, the Fe₃O₄ NPs diagram shows that the addition of this NPs has balanced the mud electrical charge, and it has established relative stability at all concentrations. At concentration above 0.027 wt. %, the extra charges of fluid neutralized, and drilling fluid became more stable. The addition of TiO₂ NPs caused a descending trend in the YP value, and this descending trend continued to the end. Also, the YP value is less than that for base mud at all NPs concentration. It indicates that the equilibrium and stability of the drilling fluid have reduced, and the deposition of NPs reduced YP, which is supported by the descending trend of PV.

3.2.3. Filtration Rate (FR) and Mud cake

Al₂O₃ negatively affects the water loss of drilling fluid. Based on the decrease in PV, it can be concluded that the addition of NPs decreases the stability of rheological properties, which this instability causes to drop in the viscosity, drop in the mud quality, and thereby increase in the water loss amount. Simultaneous investigation of water loss and PV diagrams for the Fe₃O₄ NPs shows that a decrease in the water loss and an increase in PV occur at NPs concentration of above 0.025 wt.%, which causes to improve the rheological condition of the drilling fluid. In the case of TiO₂ NPs, although at all concentrations, the fluid condition and the

rheological properties are poor, there is a proper condition in the water loss diagram.

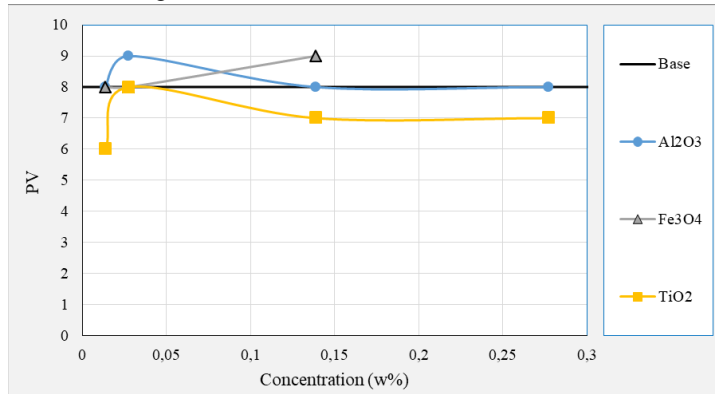


Figure 6. Effect of concentration of different NPs on PV of drilling fluid sample in different concentrations (80 pcf sample)

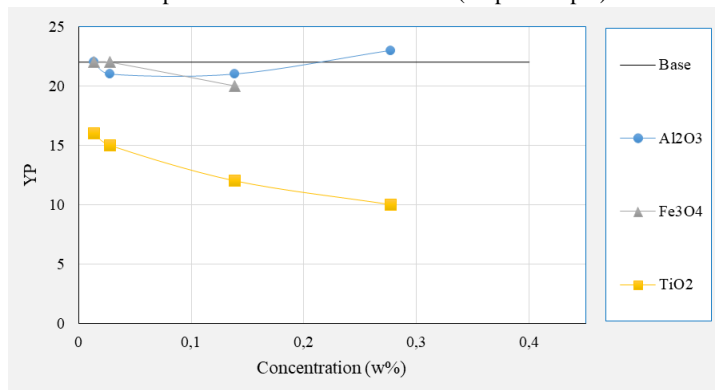


Figure 7. Effect of different NPs concentration on the drilling fluid sample variation in different concentrations (80 pcf sample)

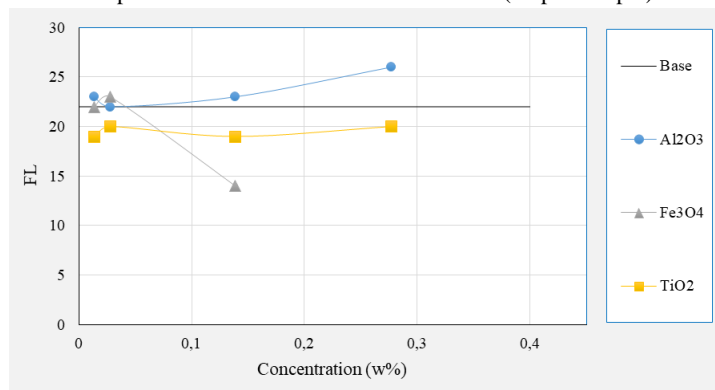


Figure 8. Effect of different NPs concentration on the filtration rate of drilling fluid sample in different concentrations (80 pcf sample)

3.3. Nanofluid circulation and invasion.

One of the most severe problems in the drilling industry is the formation damage caused by drilling fluid. Since the pressure of the drilling fluid column needs to be higher than the formation pressure in over-balance drilling, it causes the filtrate to penetrate the porous space around the well. It reduces production and causes some other problems. As a result of filtrate penetration, a mud cake is formed, which the thin and impermeable cake decreases the intensity of formation damage.

In this study, the made NP-containing fluids were tested by the formation damage apparatus, and Figures 9, 10, 11 were drawn based on the obtained data. These graphs show the pressure changes at the beginning, middle, and distance of the two ends of the core in terms of the volume of fluid injected into the core.

In the diagram of Al_2O_3 NPs, the injection started with low pressure into the formation, then pressure increased as injection continues,

and it fixed at a specific value. Pressure changes in the middle and distance of the two ends of the core are close to each other, but it differs from pressure change at the beginning of the core.

This pressure increases in diagrams A, B, C is related to the pressure changes at the beginning, end, and distance of the two ends of the core in dynamic conditions, respectively, which are associated with muds circulation within the system. Additionally, the diagrams AA, BB, CC are related to the static section of the formation damage test, which continues diagrams A, B, and C, respectively. According to the plotted diagram, it can be concluded that the penetration of the filtrate into the core was initially easy, and this penetration continued to the endpoints of the core because the core average pressure diagram and end of core pressure diagram are close to each other and are more than the pressure of the beginning of the core.

In the case of Fe_3O_4 NPs, a two-step trend is observed with an increase in pressure changes. At all three diagrams A, B, C, which represent the dynamic condition of the experiment, after the initial increase in pressure, initial stability is achieved at specific pressures. But with continued injection, the stability is broken, and an increase is observed in pressure changes again. In the static section, after a slight increase in pressure, the slope of the diagram goes to zero. According to the diagram, we can see that all three diagrams of pressure changes are close to each other. It reveals that an impermeable mud cake formed at the beginning of the core and created pressure, which caused to reduce the water loss penetration into the porous media and formation damage.

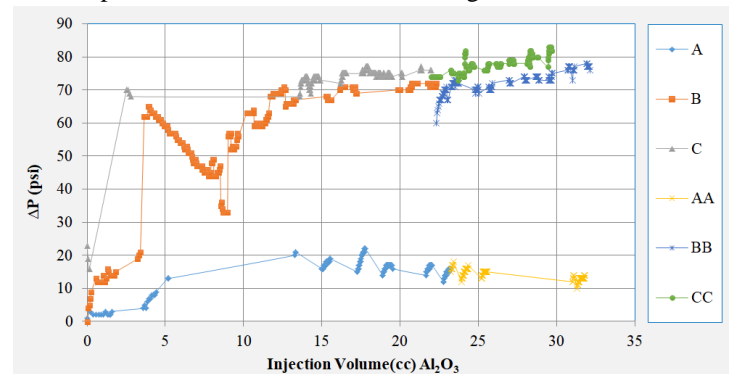


Figure 9. Pressure variations according to injection volume in the formation damage test of the sample containing Al_2O_3 NPs

In the TiO_2 NPs diagram (Figure 9), a normal increase in pressure changes to counteract the simulated pressure of the formation is initially observed. Then with overcoming the formation pressure, the fluid begins to penetrate within the core until this increase in pressure becomes constant, and the pressure does not change, as shown by the diagrams A, B, and C, which means that the dynamic section of the experiment is finished. In the static part of the experiment, the pressures become constant. Such as Al_2O_3 NPs, diagram A, representing the pressure changes at the beginning of the core, are not close to diagrams B and C, which represent the pressure changes at the end of the core and average pressure, respectively. It can be concluded that the penetration pressure is low at the beginning of the core, thereby the fluid enters the core and the pressure at the end of the core increases.

In the case of Fe_3O_4 NPs, as seen in [24], a two-step trend is observed with an increase in pressure changes. At all three diagrams A, B, C, which represent the dynamic condition of the

experiment, after the initial increase in pressure, initial stability is achieved at specific pressures. However, with continued injection, the stability is broken, and an increase is observed in pressure changes again. In the static section of the experiment, after a slight increase in pressure, the slope of the diagram goes to zero.

In Figure 10, which shows the pressure variations by injection volume in the formation damage test of specimens containing TiO₂ NPs, a normal increase in pressure changes to counteract the simulated pressure of the formation is initially observed. Then with overcoming the formation pressure, the fluid begins to penetrate within the core until this increase in pressure becomes constant and the pressure does not change, as shown by the diagrams A, B, and C, which means that the dynamic section of the experiment is finished. In the static section of the experiment, the pressures become constant.

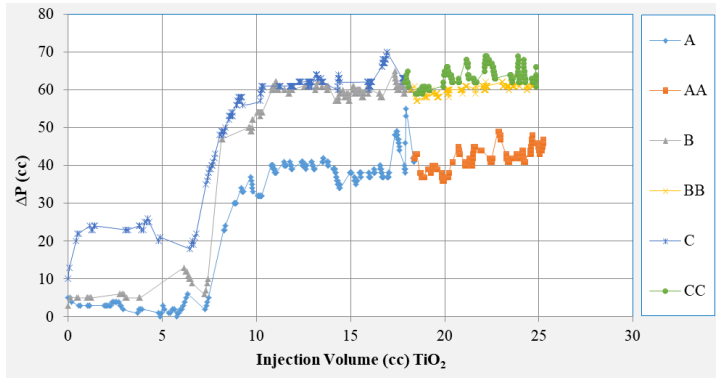


Figure 10. Pressure variations according to the injection volume in specimen damage testing of TiO₂ NPs

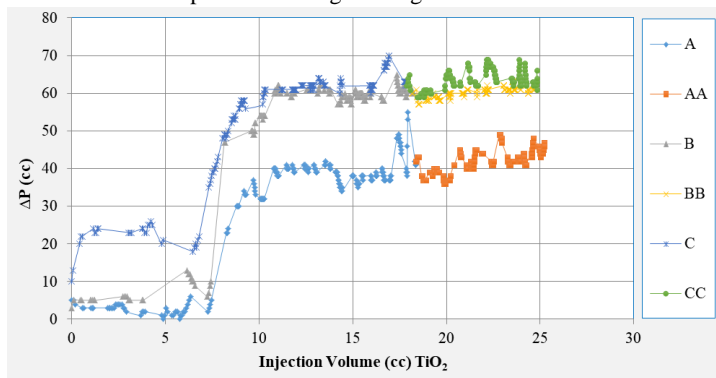


Figure 11. Pressure variations according to the injection volume in specimen damage testing of TiO₂ NPs

3.4. Permeability Reduction (k)

The most important result obtained from formation damage apparatus and formation damage diagram is the recording of initial permeability and returns permeability (after dynamic &

static MUD tests) of the core. By comparison of these two permeability, the intensity of formation damage induced by the designed drilling fluid can be obtained, which is a reasonable estimation of real condition. Depending on the ability of the NPs to improve the rheological properties of the drilling fluid, mud cakes can be formed at any point from the beginning to the end of the core by injection of fluid into the core. Therefore, the quality and position of the created mud cake are critical. It means that the stronger NPs bonds inside the drilling fluid make the microscopic bridges better and more efficient. Thereby, less filtrate penetration and formation damage occur.

In the Al₂O₃ NP experiment, to investigate the intensity of formation damage, the initial permeability was measured at three injection rates of 1, 2, 3 cc/min, and then the return permeability was calculated.

The percentage of core permeability reduction by Al₂O₃ NP is:

$$\frac{K_{Final}}{K_{Initial}} = \frac{21.63}{61.28} = 0.35 \quad (1)$$

It means that the intensity of formation damage is equivalent to the 65% reduction in initial permeability (Table 5).

The Fe₃O₄ NP sample also treated in a similar manner, which the results of the test are shown in Table 6.

The percentage of core permeability reduction by Fe₃O₄ NP is:

$$\frac{K_{Final}}{K_{Initial}} = \frac{28.28}{61.28} = 0.46 \quad (2)$$

In other words, the formation damage intensity is equivalent to 54% reduction in the initial core permeability.

By repeating the same experiment for the TiO₂ NP, the following results obtained in Table 7.

Using the data in Table 7, the percentage of core permeability reduction by TiO₂ NP is:

$$\frac{K_{Final}}{K_{Initial}} = \frac{21.63}{73.54} = 0.29 \quad (3)$$

This means that the formation damage intensity is equivalent to 71% reduction in the initial permeability.

According to the formation damage diagrams, as expected, Fe₃O₄ NPs showed the least damage compared to the two other NPs by making more suitable mud cake at the beginning of the core. The Fe₃O₄ NPs create bridges in the entrance of the core by forming bonds between the fluid components; thereby an impermeable mud cake is formed causing less filtration and consequently less formation damage [30].

Table 5. Formation damage and permeability reduction test data in Al₂O₃ NPs

Initial permeability				Return permeability (after dynamic & static MUD tests)			
Rate (cc/min)	1	2	3	Rate (cc/min)	1	2	3
DPT (psi)	7	10	13	DPT (psi)	15	24	32
Permeability (mD)	61.28			Permeability (mD)	21.63		

Table 6. Data on permeation damage testing and permeability reduction in samples containing Fe₃O₄ NPs

Initial permeability				Return permeability (after dynamic & static MUD tests)			
Rate (cc/min)	1	2	3	Rate (cc/min)	1	2	3
DPT (psi)	7	10	13	DPT (psi)	11	18	24
Permeability (mD)	61.28			Permeability (mD)	28.28		

Table 7. Data on damage testing and permeability reduction in samples containing TiO₂ NPs

Initial permeability	Return permeability (after dynamic & static MUD tests)						
Rate (cc/min)	1	2	3	Rate (cc/min)	1	2	3
DPT (psi)	7	9	12	DPT (psi)	14	32	31
Permeability (mD)	73.54			Permeability (mD)	21.63		

4. CONCLUSIONS

Experiments on the 70 pcf water-based mud that has been mixed at laboratory conditions showed that rheological properties of all nanofluids underwent relative improvements compared to the base mud. This indicates an increase in the level of interparticle forces and the strengthening of ionic bonds, which lead to higher stability in the nanofluid. Among the nanofluids, the ferrite oxide mixture demonstrated the best refinement in terms of rheological properties (Pv, Yp and Gs). Moreover, the iron oxide nanofluid led to an increasing trend in filtration measurements at all concentrations. This most probably results from the better stability of the ferrite oxide nanofluid and the establishment of a thinner and less permeable mud cake.

Experiments on the 80 pcf water-based mud that has been mixed at field conditions also point to the fact that ferrite oxide

nanoparticles improve the rheological properties of the fluid, although the effect is much less pronounced compared to the oil-based mud. Aluminum oxide and titanium oxide nanofluids did not leave significant effects on mud rheology, which may be attributed to improper field mixing. Concerning the filtration, only the iron oxide nanofluid produced positive effects for the same reasons stated above.

Formation damage studies showed that filtration invasion into the core by the ferrite oxide nanofluid was accompanied by a rise in pressure from the early stages. This is a clear sign that a thin and impermeable mud cake has been created. Hence, this nanofluid produced the smallest formation damage leading to a 56% drop in initial permeability, compare to other nanofluids.

5. REFERENCES

- Kaur, A.; Chauhan, R.P. Effect of gamma irradiation on electrical and structural properties of Zn nanowires. *Radiation Physics and Chemistry* **2014**, *100*, 59-64, <https://doi.org/10.1016/j.radphyschem.2014.03.027>.
- Mohammadzadeh, M.; Pourabbas, B.; Mahmoodian, M.; Foroutani, K.; Fallahian, M. Facile and rapid production of conductive flexible films by deposition of polythiophene nanoparticles on transparent poly(ethyleneterephthalate): Electrical and morphological properties. *Materials Science in Semiconductor Processing* **2014**, *20*, 74-83, <https://doi.org/10.1016/j.mssp.2013.12.032>.
- Moradkhani, M.R.; Karimi, A.; Negahdari, B. Nanotechnology application to local anaesthesia (LA). *Artificial Cells, Nanomedicine, and Biotechnology* **2018**, *46*, 355-360, <https://doi.org/10.1080/21691401.2017.1313263>.
- Hashemi, R.; Nassar, N.N.; Pereira Almaso, P. Nanoparticle technology for heavy oil in-situ upgrading and recovery enhancement: Opportunities and challenges. *Applied Energy* **2014**, *133*, 374-387, <https://doi.org/10.1016/j.apenergy.2014.07.069>.
- Sabeela, I.N.; Almutairi, M.T.; Al-Lohedan, A.H.; Ezzat, O.A.; Atta, M.A. Reactive Mesoporous pH-Sensitive Amino-Functionalized Silica Nanoparticles for Efficient Removal of Coomassie Blue Dye. *Nanomaterials* **2019**, *9*, <https://doi.org/10.3390/nano9121721>.
- Arab, D.; Pourafshary, P. Nanoparticles-assisted surface charge modification of the porous medium to treat colloidal particles migration induced by low salinity water flooding. *Colloids and Surfaces A: Physicochemical and Engineering Aspects* **2013**, *436*, 803-814, <https://doi.org/10.1016/j.colsurfa.2013.08.022>.
- Zhu, N.; Ji, H.; Yu, P.; Niu, J.; Farooq, M.U.; Akram, M.W.; Udego, I.O.; Li, H.; Niu, X. Surface Modification of Magnetic Iron Oxide Nanoparticles. *Nanomaterials (Basel)* **2018**, *8*, <https://doi.org/10.3390/nano8100810>.
- Taha, N.M.; Lee, S. Nano graphene application improving drilling fluids performance. In: Proceedings of the International Petroleum Technology Conference (IPTC 18539), Doha, Qatar, 6-9 December 2015, <https://doi.org/10.2523/IPTC-18539-MS>.
- Rahmani, A.R.; Bryant, S.; Huh, C.; Athey, A.; Ahmadian, M.; Chen, J.; Wilt, M. Crosswell magnetic sensing of

- superparamagnetic nanoparticles for subsurface applications. In: Paper SPE 166140, Presented at the SPE Annual Technical Conference and Exhibition, New Orleans, Louisiana, USA, 30 September-2 October 2013, <https://doi.org/10.2118/166140-PA>.
- Rahmani, A.R.; Bryant, S.; Huh, C.; Athey, A.; Ahmadian, M.; Chen, J.; Wilt, M. Crosswell magnetic sensing of superparamagnetic nanoparticles for subsurface applications. *SPE J.* **2015**, *20*, 1067-1082. <https://doi.org/10.2118/166140-MS>
- Turkenburg, D.H.; Chin, P.T.K.; Fischer, H.R. Use of modified nanoparticles in oil and gas reservoir management. Paper SPE-157120eMS. In: Presented at the SPE International Oilfield Nanotechnology Conference, Noordwijk, The Netherlands, 2012. 12-14 June. <https://doi.org/10.2118/157120-MS>
- Qin, Z.; Jung, G.S.; Kang, M.; Buehler, M. The mechanics and design of a lightweight three-dimensional graphene assembly. *Science Advances* **2017**, *3*, <https://doi.org/10.1126/sciadv.1601536>.
- Zhang, J.; Li, L.; Wang, S.; Wang, J.; Yang, H.; Zhao, Z.; Zhu, J.; Zhang, Z. Novel micro and nanoparticle-based drillingfluids: pioneering approach to overcome the borehole instability problem in shale formation. Paper SPE-176991eMS. In: Presented at the SPE Asia Pacific Unconventional Resources Conference and Exhibition, Brisbane, Australia, November 2015; pp. 9-11. <https://doi.org/10.2118/176991-MS>
- Mahmoud, O.; Nasr-El-Din, H.A.; Vryzas, Z.; Kelessidis, V.C. Nanoparticle-based drillingfluids for minimizing formation damage in HP/HT applications. Paper SPE-178949-MS. In: Presented at SPE International Conference and Exhibition on Formation Damage Control, Lafayette, Louisiana, USA, 24-26 February 2016, <https://doi.org/10.2118/178949-MS>.
- Roohullah Qalandari, Esmatullah Qalandari. A review on the potential application of nano graphene as drilling fluid modifier in petroleum industry. 2018. ISSN (Online) 2319-183X, (Print) 2319-1821, <https://doi.org/10.1021/am2012799>.
- Hoelscher, K.P.; Young, S.; Friedheim, J.; De Stefano, G. Nanotechnology Application in Drilling Fluids, in Offshore Mediterranean Conference and Exhibition. Offshore Mediterranean Conference: Ravenna, Italy. 2013; pp. 11. <https://doi.org/10.2118/157031-MS>

17. Vryzas, Z.; Kelessidis, V.C. Nano-Based Drilling Fluids: A Review. *Energies* **2017**, *10*, <https://doi.org/10.3390/en10040540>.
18. Jung, Y.; Son, Y.H.; Lee, J.K.; Phuoc, T.X.; Soong, Y.; Chyu, M.K. Rheological behavior of clay-nanoparticle hybrid-added bentonite suspensions: specific role of hybrid additives on the gelation of clay-based fluids. *ACS Appl Mater Interfaces* **2011**, *3*, 3515-3522, <https://doi.org/10.1021/am200742b>.
19. Rafati, R.; Smith, S.R.; Sharifi Haddad, A.; Novara, R.; Hamidi, H. Effect of nanoparticles on the modifications of drilling fluids properties: A review of recent advances. *Journal of Petroleum Science and Engineering* **2018**, *161*, 61-76, <https://doi.org/10.1016/j.petrol.2017.11.067>.
20. Gerogiorgis, D.I.; Clark, C.; Vryzas, Z.; Kelessidis, V.C. Development and Parameter Estimation for a Multivariate Herschel-Bulkley Rheological Model of a Nanoparticle-Based Smart Drilling Fluid. In: *Computer Aided Chemical Engineering*. Gernaey, K.V.; Huusom, J.K.; Gani, R. Eds. Elsevier, Volume 37, 2015; pp. 2405-2410, <https://doi.org/10.1016/B978-0-444-63576-1.50095-9>.
21. Gerogiorgis, D.I.; Reilly, S.; Vryzas, Z.; Kelessidis, V.C. Experimentally validated first-principles multivariate modeling for rheological study and design of complex drilling nanofluid systems. in SPE/IADC Drilling Conference and Exhibition. The Hague, The Netherlands: Society of Petroleum Engineers. 2017, <https://doi.org/10.2118/184692-MS>.
22. Reilly, S.I.; Vryzas, Z.; Kelessidis, V.C.; Gerogiorgis, D.I. First-principles Rheological Modelling and Parameter Estimation for Nanoparticle-based Smart Drilling Fluids. In: *Computer Aided Chemical Engineering*. Kravanja, Z.; Bogataj, M. Eds. Elsevier, Volume 38, 2016; pp. 1039-1044, <https://doi.org/10.1016/B978-0-444-63428-3.50178-8>.
23. Li, D.; Hong, B.; Fang, W.; Guo, Y.; Lin, R. Preparation of Well-Dispersed Silver Nanoparticles for Oil-Based Nanofluids. *Industrial & Engineering Chemistry Research* **2010**, *49*, 1697-1702, <https://doi.org/10.1021/ie901173h>.
24. Salam, M.; Al-Zubaidi, N.; Alwasiti, A. An Enhancement in Lubricating, Rheological, and Filtration Properties of Unweighted Water-Based Mud Using XC Polymer NPs. *Journal of Engineering* **2018**, *25*, <https://doi.org/10.31026/j.eng.2019.02.07>.
25. Ismail, A.; Rashid, N.; Jaafar, M.Z.; Wan Sulaiman, W.R.; Buang, N. Effect of Nanomaterial on the Rheology of Drilling Fluids. *Journal of Applied Sciences* **2014**, *14*, 1192-1197, <https://doi.org/10.3923/jas.2014.1192.1197>.
26. Alizadeh, S.; Sabbaghi, S.; Soleymani, M. Synthesis of Alumina/Polyacrylamide nanocomposite and its influence on viscosity of drilling fluid. *International Journal of Nano Dimension* **2015**, *6*, 271-276, <https://doi.org/10.7508/IJND.2015.03.006>.
27. Amarfio, E.; Abdulkadir, M. Effect of Fe₄O₃ Nanoparticles on the Rheological Properties of Water Based Mud. *Journal of Physical Science and Application* **2015**, *5*, 7-11, <https://doi.org/10.17265/2159-5348/2015.06.005>.
28. Parizad, A.; Shahbazi, K.; Tanha, A.A. SiO₂ nanoparticle and KCl salt effects on filtration and thixotropic behavior of polymeric water based drilling fluid: With zeta potential and size analysis. *Results in Physics* **2018**, *9*, 1656-1665, <https://doi.org/10.1016/j.rinp.2018.04.037>.
29. Jalalat, P. Investigation of the effects of type and concentration of metal oxide NPs on the rheological properties of aqueous base drilling fluids. In: 4th International Conference on Oil, Gas and Petrochemicals. 2017. Tehran, Iran.
30. Parizad, A.; Shahbazi, K. Experimental investigation of the effects of SnO₂ nanoparticles and KCl salt on a water base drilling fluid properties. *The Canadian Journal of Chemical Engineering* **2016**, *94*, 1924-1938, <https://doi.org/10.1002/cjce.22575>.

DO



© 2020 by the authors. This article is an open access article distributed under the terms and conditions of the Creative Commons Attribution (CC BY) license (<http://creativecommons.org/licenses/by/4.0/>).